THE JOURNAL OF BIOLOGICAL CHEMISTRY VOL. 283, NO. 24, pp. 16332–16341, June 13, 2008

Identification of a New Urate and High Affinity Nicotinate Transporter, hOAT10 (SLC22A13)*

Received for publication, January 29, 2008, and in revised form, March 14, 2008 Published, JBC Papers in Press, April 14, 2008, DOI 10.1074/jbc.M800737200

Andrew Bahn[‡1], Yohannes Hagos[‡], Stefan Reuter[§], Daniela Balen[¶], Hrvoje Brzica[¶], Wolfgang Krick[‡], Birgitta C. Burckhardt[‡], Ivan Sabolić[¶], and Gerhard Burckhardt[‡]

From the [‡]Zentrum Physiologie und Pathophysiologie, Abteilung Vegetative Physiologie und Pathophysiologie, Humboldtallee 23, 37073 Göttingen, Germany, the [¶]Unit of Molecular Toxicology, Institute for Medical Research & Occupational Health, Ksaverska cesta 2, HR-10001 Zagreb, Croatia, and the [§]Universitätsklinikum Münster, Medizinische Klinik und Poliklinik D, Exp. Nephrologie, Domagkstrasse 3a, 48147 Münster, Germany

The orphan transporter hORCTL3 (human organic cation transporter like 3; SLC22A13) is highly expressed in kidneys and to a weaker extent in brain, heart, and intestine. hORCTL3-expressing *Xenopus laevis* oocytes showed uptake of [^{3}H]nicotinate, [^{3}H]*p*-aminohippurate, and [^{14}C]urate. Hence, hORCTL3 is an organic anion transporter, and we renamed it hOAT10. [^{3}H]Nicotinate transport by hOAT10 into *X. laevis* oocytes and into Caco-2 cells was saturable with Michaelis constants (K_m) of 22 and 44 μM, respectively, suggesting that hOAT10 may be the molecular equivalent of the postulated high affinity nicotinate transporter in kidneys and intestine. The pH dependence of hOAT10 suggests *p*-aminohippurate$^-$/OH$^-$, urate$^-$/OH$^-$, and nicotinate$^-$/OH$^-$ exchange as possible transport modes. Urate inhibited [^{3}H]nicotinate transport by hOAT10 with an IC_{50} value of 759 μM, assuming that hOAT10 represents a low affinity urate transporter. hOAT10-mediated [^{14}C]urate uptake was elevated by an exchange with L-lactate, pyrazinoate, and nicotinate. Surprisingly, we have detected urate$^-$/glutathione exchange by hOAT10, consistent with an involvement of hOAT10 in the renal glutathione cycle. Uricosurics, diuretics, and cyclosporine A showed substantial interactions with hOAT10, of which cyclosporine A enhanced [^{14}C]urate uptake, providing the first molecular evidence for cyclosporine A-induced hyperuricemia.

The kidneys represent one avenue for the secretion of a large number of charged molecules. Among these are metabolites as well as exogenous substances such as drugs and environmental toxins, which are substrates for transporters of a family called solute carrier (SLC)[2] family 22A. This transporter family consists of organic anion transporters (OATs), organic cation transporters (OCTs), and zwitterion transporters. In the last decade, many members of these three subfamilies were identified and functionally characterized (for review see Refs. 1–3). However, some proteins, which were classified under the SLC22 family, *e.g.* ORCTL3, ORCTL4, FLIPT1, or BOCT, have still not been characterized and are called orphan transporters (4).

The family of OATs (*SLC22A*) was discovered in 1997 with the cloning of the renal rat and flounder OAT1 (rOAT1 (5, 6) and fOAT (7)). Meanwhile, nine OATs were functionally identified (OAT1, OAT2 (8), OAT3 (9), OAT4 (10), Oat5 (11), Oat6 (12), OAT7 (13), Oat_v1 (14), and the urate transporter URAT1 (15)). Most of these are highly expressed in the kidneys (OAT1-OAT4, Oat5, Oat_v1, and URAT1), whereas Oat6 is only expressed in the olfactory bulb, and the recently identified human OAT7 is currently the only liver-specific OAT. The substrate panel of OATs includes important endogenous compounds like urate (15–17), prostaglandins (18), neurotransmitter and tryptophan metabolites (19, 20), sulfated steroids, and a long list of drugs such as anti-viral drugs, antibiotics, antidotes (21), or diuretics (22–24).

hORCTL3 (human organic cation transporter like 3) was first described in 1998 together with hORCTL4 on chromosome 3p21.3 and noted to be ubiquitously expressed with some preference for kidneys, small intestine, and colon as detected by Northern blot analysis (25). It was speculated that hORCTL3 may function as a polyspecific organic cation transporter in several tissues. However, protein sequence alignments of all known OCTs and OATs, including the non-classified orphan transporters listed in solute carrier family 22 (SLC22) revealed several highly conserved amino acids (data not shown). On the basis of these amino acid comparisons, we hypothesized that hORCTL3 is an organic anion transporter.

In the present paper, we have examined the properties of the orphan transporter human ORCTL3. We have found that hORCTL3 is highly expressed at the apical side of renal proximal tubule cells in a gender-dependent manner. Furthermore, we provide evidence that hORCTL3 is a urate and the first identified high affinity nicotinate exchanger in kidneys and intestine. Therefore, we renamed hORCTL3 hOAT10 (human organic anion transporter 10). Finally, we present the first molecular data for a cyclosporine A-induced hyperuricemia via elevation of urate reabsorption by hOAT10.

* The costs of publication of this article were defrayed in part by the payment of page charges. This article must therefore be hereby marked "*advertisement*" in accordance with 18 U.S.C. Section 1734 solely to indicate this fact.
[1] To whom correspondence should be addressed. Tel.: 49-551-395894; Fax: 49-551-395883; E-mail: abahn@physiol.med.uni-goettingen.de.
[2] The abbreviations used are: SLC, solute carrier; OAT, organic anion transporter; OCT, organic cation transporter; PAH, *p*-aminohippurate; CCD, cortical collecting duct; SMCT1, sodium-coupled monocarboxylate transporter; URAT1, urate transporter 1; PBS, phosphate-buffered saline; RT, reverse transcription; GAPDH, glyceraldehyde-3-phosphate dehydrogenase; BBMV, brush border membrane vesicle; BLMV, basolateral membrane vesicle; HCTZ, hydrochlorothiazide; ES, estrone sulfate.

EXPERIMENTAL PROCEDURES

Reagents—Materials used included fetal bovine serum, trypsin, and PBS from Invitrogen. Buffer ingredients and unlabeled substrates were provided by Sigma-Aldrich. [2-^{3}H]PAH (3.25 Ci/mmol) was provided by PerkinElmer Life Sciences. [8-^{14}C]Uric acid (urate) (50 Ci/mmol) and [5,6-^{3}H]nicotinic acid (nicotinate) (60 Ci/mmol) were obtained from Biotrend (Cologne, Germany).

cDNA Clone—Sequencing of the entire expressed sequence tag clone, which we purchased from the Resource Center/Primary Data Base, cloned into pSPORT6 expression vector (IMAGp998D1711455Q3; GenBank™ accession number BI517655), using an automated sequencer (Applied Biosystems, Inc., Weiterstadt, Germany) and on-line services (*e.g.* the Multiple Sequence Alignment Program) (26) revealed the complete open reading frame of the novel hOAT10.

RT-PCR Analysis—Total RNA of several different tissues (First Choice Human Total RNA panel) were obtained from Ambion (Austin, TX). Total RNA from Caco-2 cells (6 days after confluence) was prepared with SV-total RNA isolation system (Promega) according to the manufacturer's protocol. 2 μg of each total RNA was reverse transcribed in a 20-μl assay applying 200 units of Moloney murine leukemia virus RT (Promega) for 1 h at 37 °C. 4–5 μl of the respective RT was used in a PCR with hOAT10_299 (sense) 5′-CCACCGCTTCAATGAGAC-3′, hOAT10_1038 (antisense) 5′-GACTGTCCACAAACCAGAC-3′, GAPDH_334 (sense) 5′-TCACCATCTTCCAGGAGCG-3′, and GAPDH_905 (antisense) 5′-CTGCTTCACCACCTTCTTGA-3′ as a control, performing 35 cycles (for hOAT10 tissue expression), 40 cycles (for hOAT10 expression in Caco-2 cells), and 20 cycles (for GAPDH) at 94 °C for 20 s, at 55 °C (for hOAT10) or 58 °C (for GAPDH) for 30 s, and at 72 °C for 1.5 min followed by a single 10-min cycle at 72 °C for extension. RT-PCR products were electrophoresed on a 1.5% agarose gel and visualized using ethidium bromide and a computer-based documentation system (Intas, Göttingen, Germany).

Real Time PCR Analysis—Total RNA of human female kidney and cDNA from these probes were prepared as described previously (27). Real time PCR was performed using hORCTL3-specific TaqMan primers and the real time PCR kit, according to the manufacturer's protocol (Applied Biosystems, Inc.).

Antibody, SDS-PAGE, and Western Blot Analysis—An immune serum against the peptide sequence in the internal loop of the protein (amino acids 306–319, LMNQLVPEKTGPSG), which is highly conserved among the species hOAT10 (GenBank™ NP_004247 for *Homo sapiens*), rOat10 (XP_236685 for *Rattus norwegicus*), and mOat10 (NP_598741 for *Mus musculus*), was raised in chicken (BioGenes, Berlin, Germany), and the antibody (hOAT10-Ab) was affinity-purified.

Brush border (BBMV) and basolateral (BLMV) membrane vesicles from male and BBMVs from female Wistar rat kidneys were prepared as previously described (28, 29). Before use, total protein was extracted from 1 mg of each vesicle preparation, employing the NucleoSpin® RNA/protein kit (Macherey-Nagel, Düren, Germany). The final protein pellet was resolved in 200 μl of the supplied buffer, and protein concentration was determined according to the Bradford protocol (30). 50 μg of the denatured (95 °C for 5 min) protein of each vesicle probe was loaded on a 10% denaturating polyacrylamide gel followed by an electrophoretical wet transfer for 1 h at 350 mA and 4 °C using a Mini Trans blot electrophoretic transfer cell (both Bio-Rad) to a polyvinylidene difluoride membrane (Roche Applied Science). After transfer, the polyvinylidene difluoride membrane was blocked for 2 h in blocking buffer (5% nonfat dry milk in PBS) and incubated at 4 °C overnight (12–14 h) in PBS buffer containing 0.5% nonfat dry milk and hOAT10-Ab (1:500), which was blocked by the corresponding peptide (at 37 °C for 2 h) in a parallel assay as a control. The labeling was performed by applying the rabbit anti-chicken horseradish peroxidase secondary antibody (1:3000; Abcam, Cambridge, UK) for 1 h at room temperature. After three more washing steps with PBS, 0.05% Tween 20, the immunoreactive bands were visualized using the ECL Western blotting detection system (Amersham Biosciences).

cRNA Synthesis and Xenopus laevis Oocyte Injection—*X. laevis* oocytes (Nasco, Fort Atkinson, WI) of stages V and VI were isolated and defolliculated by overnight incubation at 18 °C with collagenase (Type CLSII, Biochrom KG) (0.5 mg/ml) in oocyte Ringer's solution: 90 mM NaCl, 3 mM KCl, 2 mM $CaCl_2$, 1 mM $MgCl_2$, 5 mM HEPES/Tris, pH 7.6. Subsequently, they were injected with 23 nl of water (mock) or cRNA, which was synthesized from NotI-linearized pSPORT6-hOAT10 plasmid (mMessage mMachine-SP6 *in vitro* transcription kit; Ambion, Austin, TX), according to the manufacturer's protocol. Upon injection, the oocytes were incubated for 3 days at 18 °C in Barth's buffer (88 mM NaCl, 2 mM KCl, 0.82 mM $MgSO_4$, 0.66 mM $NaNO_3$, 0.77 mM $CaCl_2$, 5 mM HEPES/NaOH, pH 7.6) containing 12 mg/liter gentamycin with daily medium changes.

Transport Measurements of hOAT10 in X. laevis Oocytes—Transport experiments were carried out 3 days after injection at room temperature for the time periods indicated in oocyte Ringer's solution unless otherwise stated in the figure legends. The oocytes were then washed in ice-cold uptake buffer and dissolved in 0.25 ml of 1 N NaOH. For *trans*-stimulation experiments, *X. laevis* oocytes were injected 3 days after cRNA or water injection with two times 23 nl of 20 mM each of *p*-aminohippurate (PAH), succinate, glutarate, pyrazinoate, L-lactate, nicotinate, glutathione, 1 mM hydrochlorothiazide (HCTZ), 100 μM cyclosporine A, or oocyte Ringer's solution as a control and the uptake of 400 μM (100 μM [^{14}C]uric acid with 300 μM cold uric acid) uric acid was determined for 1 h at room temperature.

Cell Culture and Transport Measurements—The human colon adenocarcinoma-derived intestinal epithelial Caco-2 cell line (passage 15–35; ATCC, Manassas, VA) was grown in Dulbecco's modified Eagle's medium supplemented with 20% (v/v) fetal bovine serum in plastic flasks or Petri dishes (Sarstedt, Nümbrecht, Germany) at 37 °C in a 5% CO_2 atmosphere. For transport measurements the cells were plated onto 24-well plates at a density of 2×10^5 cells/well. Transport assays were performed on confluent cell monolayers 5–6 days after confluence in Ringer solution (130 mM NaCl, 4 mM KCl, 1 mM $CaCl_2$, 1 mM $MgSO_4$, 1 mM NaH_2PO_4, 20 mM HEPES, and 18 mM glucose, pH 7.4). The cells were washed twice with 500 μl of Ringer and incubated at 37 °C in Ringer containing 25 nM [^{3}H]nicotinate and the test substances for 3 min. In all of the

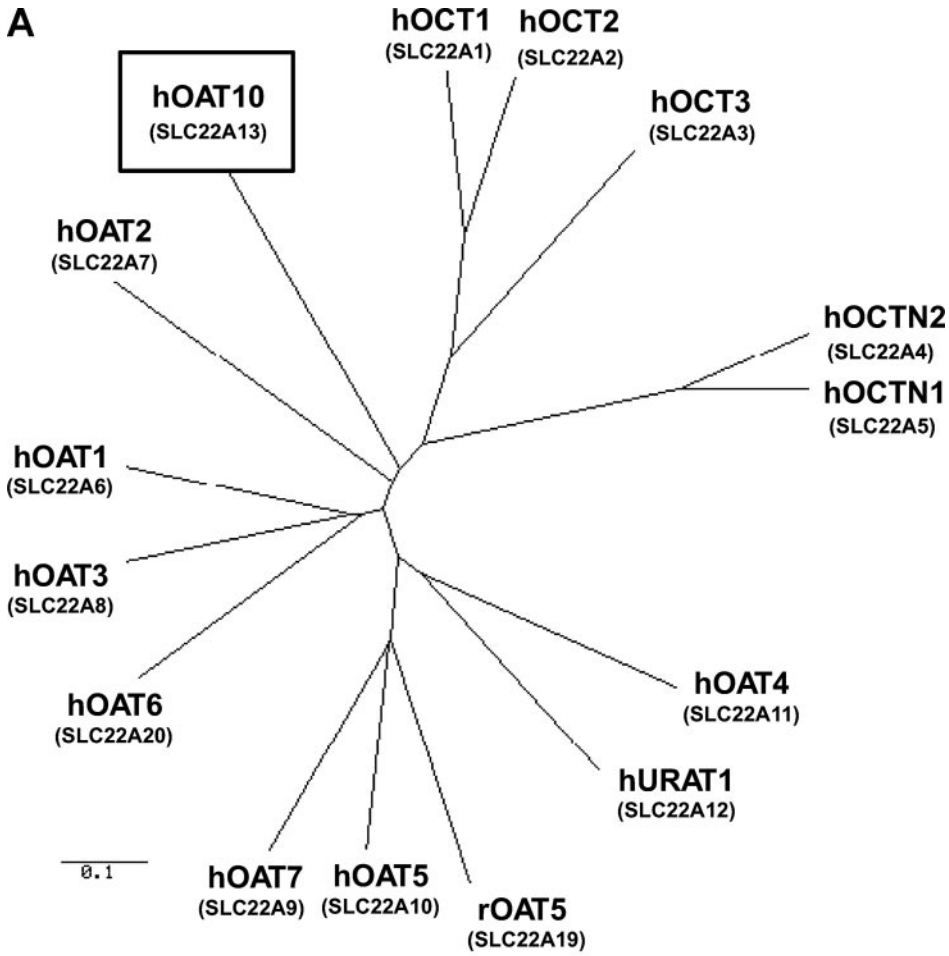

B

```
                *         20         *         40         *         60         *
hOAT10 : MAQFVQVLAEIGDFGRFQIQLLILCVLNFLSPFYPFAHVFMVLDEPHHCAVAFVKNHTFNLSAAEQLVL :  70
mOAT10 : MAQFAQVMAEVGDFGRFQVRLLILMGINFLAAFFTFGQVFMVLDEAHHCSVSWVKNHTFNLSAAEQLAI :  70
rOAT10 : MAQFAQVMAEVGDFGPFQVRVTILMGINFLSAFFVFSQVFMVLDEAHHCNVSWVKNHTFNLSAAEQLAV :  70

                80         *         100        *         120        *         140
hOAT10 : SVFLDTAGPPECLMFRPPPANASLQDILSHRFNETQPCDMGWEYPENRLPSLKNEFNLVCDRHLKDTT : 140
mOAT10 : SIPNDTTGRPESCLMFRPPPDSASLEDILSHRFNETQACDSGWDYPENRPGSLKKEFDLVCDRNLKRTS : 140
rOAT10 : SIPNDTAGRPESCLMFRPPPDSASLEDILSHRFNETQACDSGWDYPENRPPSLKNEFDLVCDRENLKRTS : 140

                *         160        *         180        *         200        *
hOAT10 : QSVFMGGLLVGALMFGPLCDRIGRKATILAQLLLFTLIGLATAFVPSFELYMALRFAVATAVAGLSFSNV : 210
mOAT10 : QSVFMAGLLVGALVFGPVCDRIGRRPSLLMQVLLSGITSMATAFVSSFELYLALRFVLATANAGFLLSTN : 210
rOAT10 : QSVFMAGLLVGALVFGPVCDRIGRRPSLLMQLLLSGIASMATAFVSSFELYMTLRFALATANAGFLLSSN : 210

                220        *         240        *         260        *         280
hOAT10 : TLLTEWVGPSNRTQAVVLAQCNFSLGQMVLAGLAYGRNWRLLQITGTAPGFLLLFYFWALPESARWLLT : 280
mOAT10 : VLISEWVGPSNRTQAVVLAQCNVALGQMVLAGLAYGVRNWRLLQITGTAPVLLLLFYFWVLPESPRWLLS : 280
rOAT10 : VLLSEWVGTSNRTRAMVLAQSNFALGQMALAGLAYGVRNWRLLQITGTPPFLLVFYFWVLPESPRWLLS : 280

                *         300        *         320        *         340        *
hOAT10 : RGRMDSAIQLIQKAASVNRRRLSPELMNQLVPEKTGPSGNALDLFRHPQLRKVTLIIFCVWFVDSLGYYG : 350
mOAT10 : QGRTEEAKQLVQKAALVNGRFLSPELLNQLVPEKTGPSGNALDLFRHPHLRKVTLILLAVWFVDSLVYYS : 350
rOAT10 : QGRTEEAKQLVQKAALVNGRFLASELLNQLVPEKTGPSGNALDLFRHPQLRKVTLILLAVWFVDSLLYYS : 350

                360        ^         380        ^         400        ^         420
hOAT10 : LSLQVGDFGLDVYLTQLIFGAVEVPARCSSIPMMQRLGRKWSQLGTLVLCGLMGIIIIFIPADLPVVTM : 420
mOAT10 : LSFQVGDFGLDIYVTQLIFGAVEMPGRFLSVLMMEKLGRKWSQLETLTLAGIMIIIIFIPGDLPTVTV : 420
rOAT10 : LGLQVGDFGLDIYLTQVIFGVVEVPARLSSIPMMEKLGRKWSQLETLTLAGVMCVIIIFIPGDLPTVAL : 420

                *         440        *         460        *         480        *
hOAT10 : LAVVGRMATAAAFTISYVYSAELFPTILRQTGMGLVGIFSRIGGILTPLVILLGEYHAALPMLIYGSLPI : 490
mOAT10 : LAVVGKFASAAAFTISYVYTAELFPTIIRQTGMGLVSIFSRVGGIITPLVMLLEQYHCAIPMVIFGSLPI : 490
rOAT10 : LAVVGKFASSAAFTISYVYTAELFPTIIRQTGMGLVSIFSRVGGIITPLVMLLEQYHCAIPMLIFGSLPI : 490

                500        *         520        *         540        *
hOAT10 : VAGLLGTLLPETHGQGLKDTLQDLEGPHPRSPKSVPSETRAGRTSSPGVAEVESTYF : 551
mOAT10 : GAGLLCALLPETRGQTLKDTLQDLEQGLPAGSHKTAPQRQDMEASGRTSSVEVAVVKSSYF : 551
rOAT10 : GAGLLCALLPETRGQTLKDTLQDLEQGPPRSHKTAPQRKDVEASGRTSSAEVAVVKSSYF : 551
```

FIGURE 1. **Homology of hOAT10 within the SLC22A family.** *A*, phylogenetic tree of the solute carrier family 22A illustrating the relation of hOAT10 to the other family members. *B*, sequence alignment of OAT10 orthologs from human, rat, and mouse.

experiments, the ^{3}H and ^{14}C contents were determined after neutralization of the probes with 0.25 ml of 1 N HCl by liquid scintillation counting (Canberra-Packard, Dreieich, Germany).

Kinetic and Statistical Analysis—For the determinations of the urate concentrations that blocked 50% of [^{3}H]nicotinate uptake (IC_{50}), the Equation 1 was used and fitted by nonlinear regression with SigmaPlot 2006 (SPSS Science, Chicago, IL).

$$v = \frac{v_0}{1 + \left(\frac{I}{IC_{50}}\right)^h} \quad \text{(Eq. 1)}$$

v is the rate of [^{3}H]nicotinate uptake in the presence of the inhibitor (urate), v_0 is the rate of [^{3}H]nicotinate uptake in the absence of the inhibitor (in this case set to 100%), I is the inhibitor concentration, and h is the Hill coefficient representing the cooperativity between the tested substances and the transporter.

The hOAT10-specific uptake of [^{3}H]nicotinate (*i.e.* transport in oocytes minus that observed in mock) was a saturable function of substrate concentration that was adequately described by the Michaelis-Menten equation (Equation 2) for competitive interaction of labeled and nonlabeled substrate (31),

$$J = \frac{J_{max}[*S]}{K_t + [*S] + [S]} + C \quad \text{(Eq. 2)}$$

where J is the rate of [^{3}H]nicotinate transport from a concentration of labeled substrate equal to [*nicotinate], J_{max} is the maximum rate of mediated [^{3}H]nicotinate transport, $K_t = K_m$ is the nicotinate concentration that results in half-maximal transport (apparent Michaelis constant), [S] is the concentration of unlabeled nicotinate in the transport reaction, and C is a constant that represents the component of total nicotinate uptake that is constant (over the range of substrate concentrations tested) and presumably reflects the combined influence of diffusive flux, nonspecific binding, and/or incomplete rinsing of the cell layer. Unpaired Student's t test was used to assess differences between two groups. Statistical analysis and grafical layout were performed with Microsoft Excel (Microsoft, Unterschleissheim, Germany) and SigmaPlot 2006 (SPSS Science, Chicago, IL).

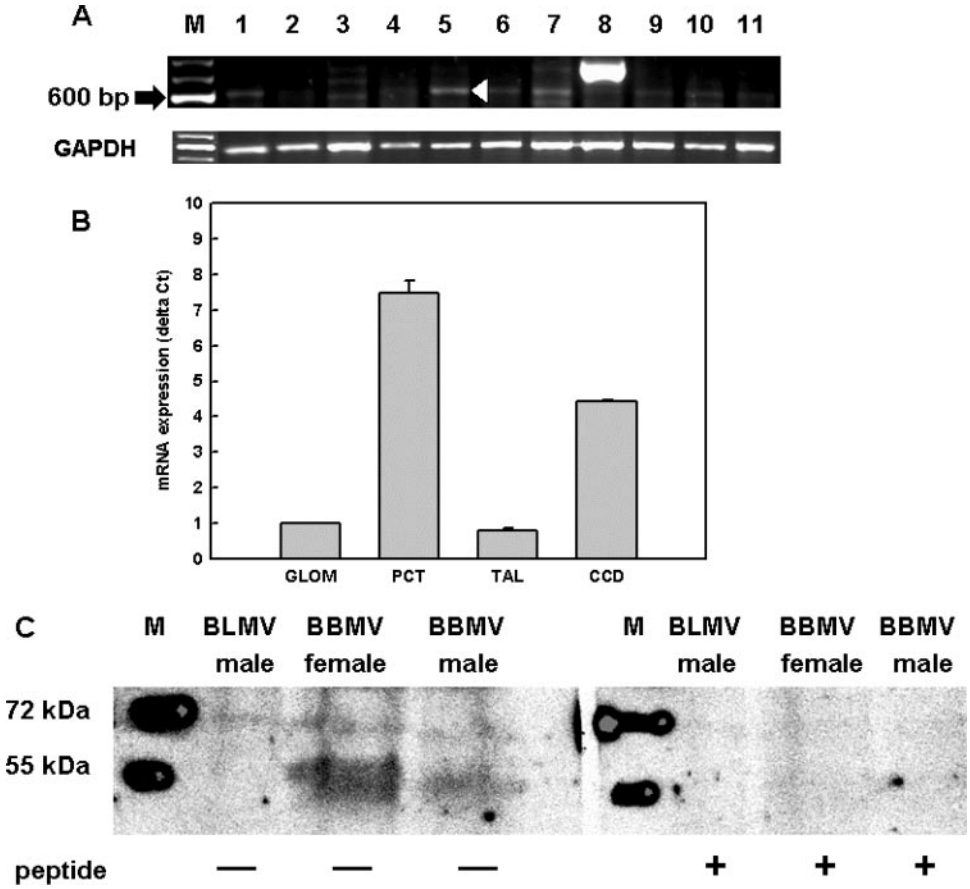

FIGURE 2. **Analysis of hOAT10 expression.** *A*, 1.5% agarose gel of a RT-PCR analysis of hOAT10 tissue distribution using total RNA from several tissues, including adipose (*lane 1*), bladder (*lane 2*), brain (*lane 3*), cervix (*lane 4*), colon (*lane 5*), esophagus (*lane 6*), heart (*lane 7*), kidney (*lane 8*), liver (*lane 9*), lung (*lane 10*), and ovary (*lane 11*); *Lane M* represents the molecular mass marker, and the *white arrow* documents one of three splice variants of hOAT10. Expression of GAPDH was determined in parallel as control. *B*, real time PCR analysis of nephron segments of female human kidney; *GLOM*, glomerulus; *PCT*, proximal convoluted tubule; *TAL*, thick ascending limb. *C*, Western blot analysis of protein extracts of BBMVs and BLMVs from rat kidney. Immunostaining of rOat10 was performed with hOAT10-Ab with or without preincubation with the corresponding peptide. *Lane M* represents the molecular mass protein marker.

RESULTS

For all of the studies an expressed sequence tag clone (GenBank™ accession number BI517655) was used, including the entire open reading frame of the orphan transporter hORCTL3 (SLC22A13), which consists of 1656 bp, coding for 551 amino acids with a homology of 44% to hOAT1. Because OAT8 and OAT9 were already mentioned in the literature without a clear definition of their sequence or relation to the SLC22 family (3), we changed hORCTL3 to hOAT10, because of its characteristics, which are to be discussed later. A comparison of hOAT10 with all characterized members of the SLC22 family is provided in the phylogenetic tree (Fig. 1*A*), documenting that hOAT10 constitutes its own branch and exhibits only weak homologies to the other members of the SLC22 family. Further BLAST searches have explored orthologs also from the rat (XP_236685, 72% identity) and the mouse (NP_598741, 72% identity) (Fig. 1*B*).

An examination of the tissue distribution using a panel of total RNA revealed a strong expression of the full-length hOAT10 variant in the kidneys and weaker signals in brain, heart, and colon (Fig. 2*A*). Additionally, we detected several splice variants of hOAT10, which we confirmed by the cloning and sequencing of additional bands visible in Fig. 2*A* (*white arrow*) and Fig. 10 below the full-length hOAT10 PCR product (*white arrow*), resulting mostly in a loss of exon three and of a part or all of exon 4 (data not shown). These splice variants were detected in many organs, indicating a more ubiquitous expression of hOAT10 (see Figs. 2*A* and 10). Real time PCR measurements in different nephron segments of female kidney defined high expression of hOAT10 in proximal convoluted tubule and interestingly also in cortical collecting duct (CCD), whereas glomerulus and thick ascending limb exhibited virtually no expression of hOAT10 (Fig. 2*B*).

To further prove hOAT10 localization in rat or human kidney, we raised an antibody against a conserved region, an internal loop at amino acid positions 306–319, in chicken. Several trials to document OAT10 expression in the kidney by immunohistochemistry failed (data not shown). Alternatively, we tested whether OAT10 is expressed in the apical or basolateral membrane of tubular epithelial cells using rat BLMVs and BBMVs. Western blot analysis of protein extracts of these vesicles showed a clear cut detection of a band at 55 kDa in BBMV, which was blocked by the corresponding peptide (Fig. 2*C*). This molecular mass of hOAT10 correlates well with the calculated protein mass of 61 kDa. No band was visible in BLMV, suggesting that renal hOAT10 expression is restricted to the apical membrane. A comparison of OAT10 expression in male and female BBMVs, loading the gel with 50 μg of protein each, showed a female over male dominance (Fig. 2*C*).

A functional characterization of hOAT10 was explored in *X. laevis* oocytes. hOAT10-expressing oocytes exhibited substantial uptakes of [^{3}H]*p*-aminohippurate (137.4 ± 8.8 *versus* 29 ± 1.6 fmol/oocyte for 30 min; Fig. 3*A*), [^{14}C]urate (3.2 ± 0.2 *versus* 0.8 ± 0.04 pmol/oocyte for 30 min; Fig. 3*B*), and [^{3}H]nicotinate (64.3 ± 4.7 *versus* 7.3 ± 0.6 fmol/oocyte for 30 min; Fig. 3*C*) each compared with mocks. Transport of [^{3}H]nicotinate was time-dependent and reasonably linear for 60 min (data not shown); 30 min was used for all kinetic studies of nicotinate transport. hOAT10-mediated nicotinate uptake was saturable with a Michaelis constant (K_m value) of 22 ± 14.1 μM (n = 3), indicating that hOAT10 is a high affinity nicotinate transporter (Fig. 4). To evaluate the affinity of hOAT10 for urate, we performed an IC_{50} determi-

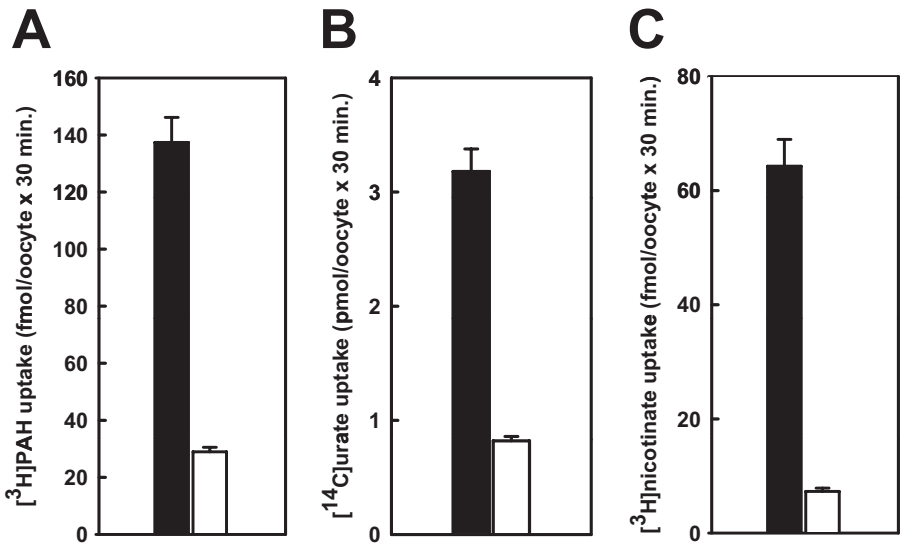

FIGURE 3. **Transport of *p*-aminohippurate, urate, and nicotinate by hOAT10.** 1 μM [^{3}H]PAH (*A*), 50 μM [^{14}C]urate (*B*), and 25 nM [^{3}H]nicotinate (*C*) uptake for 30 min at room temperature into *X. laevis* oocytes expressing hOAT10 (*black bars*) in comparison with water-injected oocytes (*white bars*). The *bars* are the means (±S.E.) of uptakes determined in three separate experiments with 8–11 oocytes each.

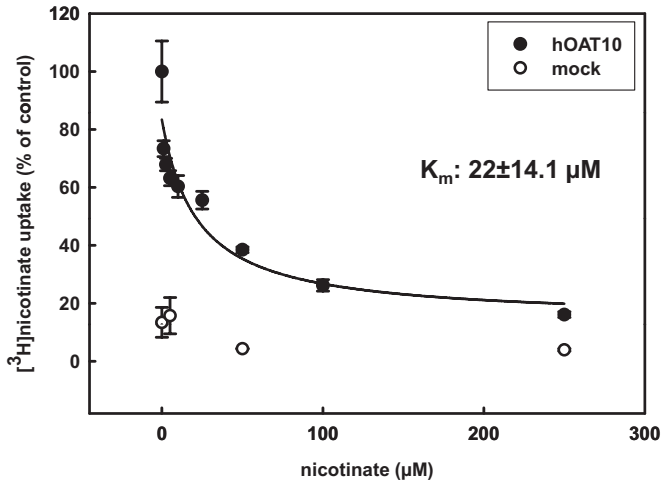

FIGURE 4. **Kinetic analysis of nicotinate uptake by hOAT10.** The effect of unlabeled nicotinate on the uptake of 25 nM [^{3}H]nicotinate into hOAT10-expressing *X. laevis* oocytes and into water-injected (mock) oocytes measured for 30 min at room temperature and pH 5.0. The points are the means (±S.E.) of uptakes determined in three separate experiments with 8–11 oocytes each. The *line* was based upon a nonlinear regression algorithm employing Equation 2.

nation with nicotinate as a substrate. The urate concentration inhibiting 50% of maximal nicotinate transport was 759 ± 501 μM, consistent with hOAT10 being a low affinity urate transporter like hOAT4 in comparison with the classical urate transporter hURAT1 (16) (Fig. 5).

Inhibition of hOAT10-mediated PAH (1 μM) transport revealed a significant reduction of PAH uptake by urate (82.5 ± 4%) and salicylate (80.7 ± 3%) and highly significant inhibitions for estrone sulfate (ES, 38.8 ± 3%) and the classical inhibitor of organic anion transport probenecid (57.7 ± 3.5%), whereas reduced GSH and the typical substrate of organic cation transporters, tetraethylammonium, did not alter PAH transport, confirming that hOAT10 is an OAT (Fig. 6). Despite the abolishment of PAH uptake by ES, hOAT10 did not transport radioactively labeled ES (data not shown).

To examine the pH dependence of hOAT10-mediated transport, we employed PAH as a substrate that does not change its charge over the applied pH ranges. Acidification of the uptake medium to pH 5.0 led to a more than 2-fold (219 ± 13.5%) increase in [^{3}H]PAH uptake compared with the PAH uptake at pH 7.4, which was set at 100%. Alkalization of the medium to pH 8.5 resulted in a significant ($p < 0.01$) inhibition of PAH uptake to 63.4 ± 4.8% (Fig. 7), indicating a marked pH dependence of hOAT10.

An inhibition study on hOAT10-mediated [^{14}C]urate uptake, using 1 mM each of succinate, L-lactate, pyrazinoate, nicotinate, glutarate, and, as a control, probenecid, significantly reduced urate uptake by 22–50% (Fig. 8*A*). To investigate whether any of these compounds is translocated, we injected each of these substances in a concentration of 20 mM into hOAT10-expressing oocytes and measured [^{14}C]urate uptake. We found a significant *trans*-stimulation of 24–39% for all substances with the exception of glutarate, suggesting that hOAT10 facilitates also urate$^-$/PAH$^-$, urate$^-$/succinate^{2-}, urate$^-$/pyrazinoate$^-$, urate$^-$/L-lactate$^-$ as well as urate$^-$/nicotinate$^-$ exchange (Fig. 8*B*).

Next we tested the interaction of hOAT10 with several uricosurics, diuretics, and the immune suppressive agent cyclosporine A, some of which are known to cause hyperuricemia. All of the compounds reduced [^{3}H]nicotinate uptake substantially by 33–62%, indicating that they may reduce urate or nicotinate reabsorption also *in vivo* (Fig. 9*A*). An examination of the *trans*-stimulatory effect of HCTZ and cyclosporine A revealed significantly enhanced urate uptake by hOAT10-expressing oocytes for cyclosporine A (164 ± 28.2). HCTZ did not change hOAT10-mediated urate uptake in comparison with the documented *trans*-stimulation of urate uptake by nicotinate (Fig. 9*B*). Additionally, we tested the *trans*-effect of reduced GSH on hOAT10-mediated urate uptake. We note for the first time that GSH is translocated by an OAT, namely hOAT10, driving urate uptake by a factor of more than 2 (244 ± 42%).

Recently, it was documented that human intestinal vesicles as well as Caco-2 cells express a high affinity nicotinate transporter (32). We first tested the expression of hOAT10 by RT-PCR in Caco-2 cells. Using male and female total RNA of the kidney and the pSPORT6-hOAT10 plasmid as a control, we detected several splice variants of hOAT10 in Caco-2 cells, including the full-length variant that we used in this study for functional characterization (Fig. 10). An evaluation of the apparent Michaelis constant (K_t value; Equation 2) for nicotinate in Caco-2 cells, which was carried out with [^{3}H]nicotinate at

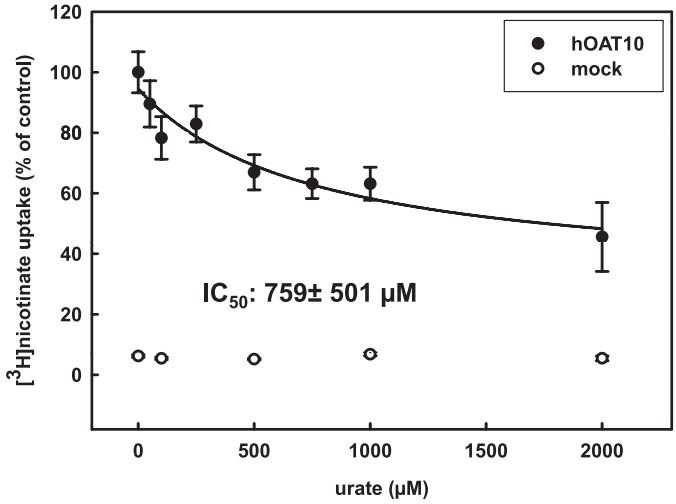

FIGURE 5. **IC_{50} determination for urate *versus* nicotinate for hOAT10.** The concentration dependence of hOAT10-mediated uptake of 25 nM [^{3}H]nicotinate uptake in *X. laevis* oocytes applying increasing concentrations of cold urate for 30 min at room temperature is illustrated. The *open circle* represents the uptake of nicotinate by water-injected (mock) oocytes as a control. The data are the means (±S.E.) of uptakes determined in three separate experiments with 8–11 oocytes each. The *line* was based upon a nonlinear regression algorithm using eq. 1.

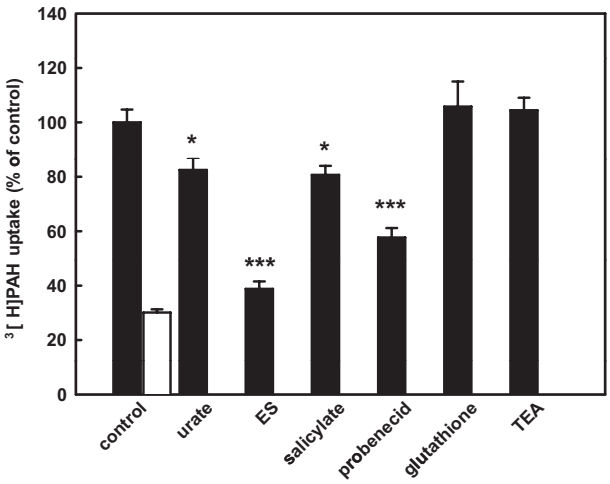

FIGURE 6. ***cis*-Inhibition profile of hOAT10 for several anionic and cationic substances.** *cis*-Inhibition study of 1 μM [^{3}H]PAH uptake into hOAT10-expressing *X. laevis* oocytes, using 1 mM of anionic and cationic substances and the classical inhibitor probenecid over 30 min at room temperature. The length of each column is calculated as a percentage of [^{3}H]PAH accumulation under control conditions (control = 100%) measured without inhibitor. The value for water-injected oocytes (*white bar*) represents the mean of all examined water-injected oocytes (mean ± S.E.; $n = 3$ independent experiments with 8–11 oocytes each). *TEA*, tetraethylammonium. *, $p < 0.05$; ***, $p < 0.001$ *versus* control.

pH 5.0 for 3 min at 37 °C according to the published conditions, revealed a value of 48.4 ± 33.6 μM consistent with an involvement of hOAT10 in intestinal nicotinate uptake (Fig. 11).

DISCUSSION

A re-evaluation of the tissue distribution of the orphan transporter hORCTL3 by RT-PCR revealed a strong expression in kidneys, indicating hORCTL3 to be a kidney-specific transport protein. Moreover, we found weaker expressions of different splice variants of the open reading frame of hORCTL3 especially in brain, heart, and colon, supporting the previous findings of a more general expression of hORCTL3 (25). A detailed picture of the renal expression of hORCTL3 was determined by real time PCR of isolated segments of a human female nephron such as the glomerulus, the proximal convoluted tubule, the thick ascending limb, and the CCD. Surprisingly, we detected hORCTL3 not only in the proximal convoluted tubule but also in the CCD.

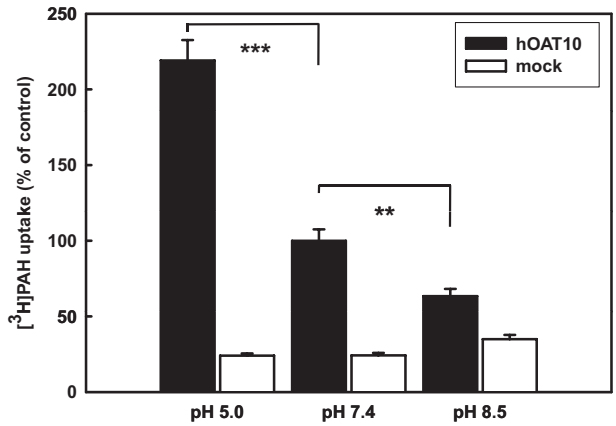

FIGURE 7. **pH dependence of hOAT10-mediated [^{3}H]PAH uptake.** Uptake of 1 μM [^{3}H]PAH was examined at different pH conditions of the transport medium over 30 min at room temperature. The *black columns* represent hOAT10-expressing *X. laevis* oocytes, and the *white columns* represent water-injected (mock) oocytes. The data points were normalized by setting the values of hOAT10-expressing oocytes at pH 7.4 as a control to 100%. Each value represents the means ± S.E. of three independent experiments with 8–11 oocytes each. **, $p < 0.01$; ***, $p < 0.001$ *versus* control.

To confirm these PCR results and to explore the membrane localization of hORCTL3, we raised an antibody against a highly conserved internal loop of hORCTL3 in chicken. Unfortunately, this antibody did not show any immune reaction in rat or human kidney tissues. However, Western blot analysis using BBMVs or BLMVs of rat kidney demonstrated an expression of rOrctl3 at the luminal side of proximal tubule cells. This was expected, because ORCTL3 possesses a PDZ domain motif at the C-terminal end, similar to other apical OATs such as hOAT4 or hURAT1 (33, 34). A further comparison of male and female BBMVs suggested a gender dependence of ORCTL3 expression with a dominant female over male expression, similar to that described recently for rat organic anion transporter 2 (35). Other transporters such as Oat1, Oat3, and URAT1 showed male over female dominance (36, 37). Gender-specific constellations of transport proteins may result in gender-specific reabsorption as well as secretion of organic anions such as endogenous metabolites or drugs (38).

This is the first report of an apical organic anion transporter in CCD. Recently, we demonstrated mouse Oat3 expression on the basolateral side of the whole nephron. The concept of basolateral prostaglandin E_2 release in macula densa cells via OAT3 may also be realized in CCD cells. Prostaglandin E_2 regulates adenylate cyclase activity of CCD cells, leading to a down-regulation of water transport by aquaporin 2 (20, 39). Based on our findings, we have to consider organic anion transport (reabsorption as well as secretion) additionally in CCD. Possible substrates for hORCTL3 in CCD include prostaglandins (*e.g.* prostaglandin E_2) and urate. Further experiments are necessary to

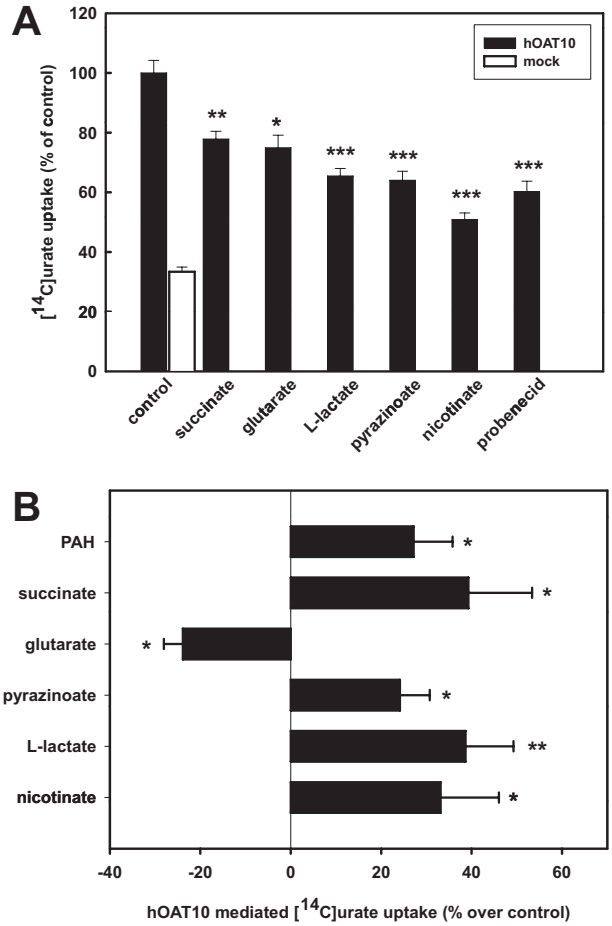

FIGURE 8. **Specificity of hOAT10 for organic anions.** *A*, *cis*-inhibition study using 1 mM of several mono- and dicarboxylates in comparison with the classical inhibitor probenecid on the uptake of 50 μM [^{14}C]urate into hOAT10-expressing *X. laevis* oocytes over 30 min at room temperature. The length of each column is calculated as percentage of [^{14}C]urate accumulation under control conditions (control = 100%) measured without inhibitor. The value for water-injected oocytes (*white bar*) represents the mean of all examined water-injected oocytes (mean ± S.E.; $n = 3$ independent experiments with 8–11 oocytes each). *, $p < 0.05$; **, $p < 0.01$; ***, $p < 0.001$ *versus* control. *B*, *trans*-stimulation study of hOAT10-mediated [^{14}C]urate transport was determined. Three days after hOAT10-cRNA or water injection 20 mM each of PAH, succinate, glutarate, pyrazinoate, L-lactate, nicotinate, or oocyte Ringer as a control were injected, and uptake of 400 μM (100 μM [^{14}C]urate + 300 μM cold urate) urate was determined for 1 h at room temperature. The *black columns* show hOAT10-mediated [^{14}C]urate uptake (mean ± S.E.; $n = 3$ independent experiments with 5–7 oocytes each). *, $p < 0.05$; **, $p < 0.01$ *versus* control.

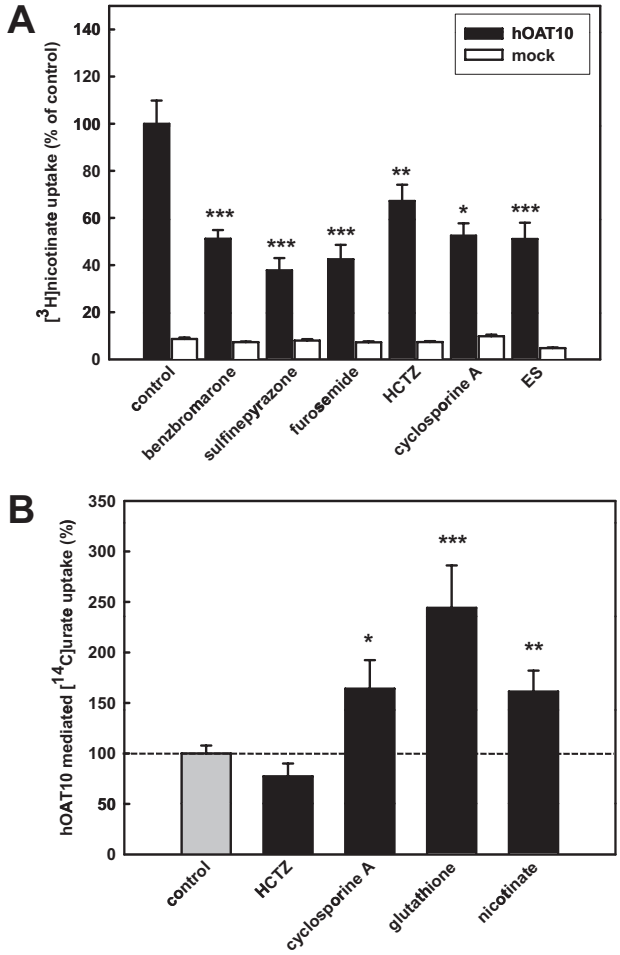

FIGURE 9. **Specificity of hOAT10 for uricosurics, diuretics, and cyclosporine A.** *A*, *cis*-inhibition study of 25 nM [^{3}H]nicotinate uptake into hOAT10-expressing *X. laevis* oocytes, employing uricosurics (50 μM benzbromarone and 1 mM sulfinepyrazone), diuretics (1 mM furosemide and 1 mM HCTZ), 100 μM cyclosporine A, and 1 mM ES as a control over 30 min at room temperature. The length of each column is calculated as a percentage of [^{3}H]nicotinate accumulation under control conditions (control = 100%) measured without inhibitor. The *white bars* represent water-injected oocytes (mock cells). All of the tested substances excluding HCTZ and cyclosporine A showed highly significant ($p < 0.001$) inhibition of [^{3}H]nicotinate transport (mean ± S.E.; $n = 3$ independent experiments with 8–11 oocytes each). *, $p < 0.05$; **, $p < 0.01$; ***, $p < 0.001$ *versus* control. *B*, *trans*-stimulation study of hOAT10-mediated [^{14}C]urate transport was determined. Three days after hOAT10-cRNA or water injection 20 mM each of glutathione or nicotinate, 1 mM HCTZ, 100 μM cyclosporine A, or oocyte Ringer as a control were injected and uptake of 400 μM (100 μM [^{14}C]urate + 300 μM cold urate) urate was determined for 1 h at room temperature. The *gray column* represents hOAT10-mediated urate uptake after oocyte Ringer injection. The *black columns* show hOAT10-mediated [^{14}C]urate uptake (mean ± S.E.; $n = 2$ independent experiments with 5–7 oocytes each). *, $p < 0.05$; **, $p < 0.01$; ***, $p < 0.001$ *versus* control.

evaluate the role of organic anion transport and therefore of OAT3 as well as ORCTL3 in cortical collecting ducts.

To address our hypothesis that hORCTL3 belongs to the OATs, a functional evaluation of hORCTL3 was performed by uptake of several organic anions, including PAH, urate, nicotinate, and ES in hORCTL3-expressing *X. laevis* oocytes. The substantial uptake of PAH, urate, and nicotinate compared with water-injected oocytes constitutes the first proof that hORCTL3 is an organic anion transporter. An inhibition of PAH uptake by ES, salicylate, and probenecid and no alteration of PAH uptake by tetraethylammonium reflect typical characteristics of members of the OAT family (1, 3, 24). Consequently, and because of the lack of the molecular identity of OAT8 and OAT9 (3), we renamed this transporter hOAT10 (human organic anion transporter 10).

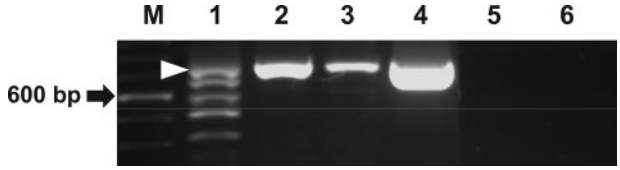

FIGURE 10. **Analysis of hOAT10 expression in Caco-2 cells.** 1.5% agarose gel of a RT-PCR analysis of hOAT10 expression in Caco-2 cells is shown. *Lane M* represents the molecular mass marker, and the *white arrow* documents the full-length variant of hOAT10. Total RNA from male (*lane 2*) and female (*lane 3*) human kidney and hOAT10-pSPORT6 plasmid (*lane 4*) were used as positive controls. *Lanes 5* and 6 show negative controls.

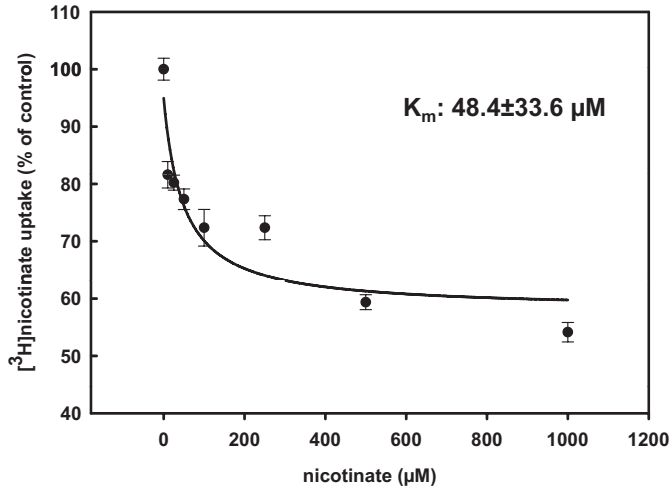

FIGURE 11. **Kinetic analysis of nicotinate uptake by Caco-2 cells.** The effect of unlabeled nicotinate on the uptake of 25 nM [^{3}H]nicotinate into Caco-2 cells for 3 min at 37 °C and pH 5.0 is documented. The points are the means (±S.E.) of uptakes determined in three separate experiments with four repeats each. The *line* was based upon a nonlinear regression algorithm employing Equation 2.

Nicotinate (niacin) is an essential vitamin (vitamin B_3), which has to be reabsorbed in the intestine from the diet or synthesized via breakdown of the essential amino acid tryptophan in the so called "kynurenine pathway" in times of low niacin supply, resulting in low nicotinate plasma concentrations of 2–4 μM. Intestinal reabsorption of nicotinate was thought to involve an anion exchange mechanism and a proton-coupled transport system (40). Recently, the sodium-coupled monocarboxylate transporter 1 (SMCT1) was documented to transport nicotinate with a relatively high affinity (K_m value of 230 μM). Because of its abundant expression in the intestine, it was presumed to be the most important transporter for nicotinate reabsorption (41).

However, Nabokina *et al.* (32) documented high affinity and sodium-independent nicotinate transport (K_m value of 0.5 μM) in the human intestinal epithelial Caco-2 cell line. Moreover, in additional experiments on brush border membrane vesicles of human jejunum, they confirmed a strict pH dependence of nicotinate reabsorption, being higher at low pH. This is consistent with our observation of a pH dependence of hOAT10, facilitating nicotinate/H^+ symport or more likely nicotinate$^-$/OH^- exchange. Furthermore, we detected hOAT10 in colon and Caco-2 cells. Comparable K_m values for nicotinate transport by hOAT10 (22 μM) expressed in *X. laevis* oocytes and for Caco-2 cells (44 μM) at pH 5.0 lead us to conclude that hOAT10 represents the postulated high affinity nicotinate transporter in Caco-2 cells and, consequently, in human intestine.

Nicotinate may serve not only for NAD^+ synthesis, which is important for energetic processes, signal transduction pathways, or even the activation of the NAD^+-dependent histone deacetylase SIRT1 and therefore life extension (42), but also for reabsorption of the purine metabolite urate.

In higher primates including man, urate is the end product of the purine metabolism, because of the loss of hepatic uricase activity. Approximately 70% of daily urate secretion occurs via the kidneys, involving reabsorption and secretion processes (43). The low fractional excretion of urate in humans (FE_{urate} = ~10%) results in high urate plasma levels of 200–500 μM, which are presumed to be an advantage during hominoid evolution, because of the scavenging properties of urate on reactive oxygene species and of its influence on blood pressure regulation (for review see Ref. 44). Nowadays, urate comes back into clinical focus, because of its impact on cardiovascular and neurodegenerative diseases (45). Transporters currently known to play a significant role on urate plasma levels have recently been identified as URAT1, Oat1, Oat3, and glucose transporter 9 (GLUT9, SLC2A9), determined via knock-out mouse models or single nucleotide polymorphisms in man (15, 46–48).

Our observation of hOAT10-mediated urate transport as well as the inhibition of nicotinate uptake by increasing concentrations of urate indicates that hOAT10 is a low affinity urate transporter possibly involved in renal urate reabsorption like hOAT4 (16). The impact of hOAT10 on urate plasma levels in man is still open, but studies on renal urate reabsorption in Urat1 knock-out mice showed that a substantial fraction is covered by a yet unknown transporter, which might be the mouse ortholog of hOAT10 (46).

A further characterization of the driving forces for urate uptake by hOAT10 to be able to differentiate between the various apical urate transporters such as URAT1, hOAT4, and Oat_v1 included preloading of *X. laevis* oocytes with L-lactate, nicotinate, or pyrazinoate. All three tested substances enhanced urate uptake by hOAT10, indicating urate$^-$/L-lactate$^-$, urate$^-$/nicotinate$^-$, as well as urate$^-$/pyrazinoate$^-$ transport modes of hOAT10 similar to hURAT1 (15), but different to hOAT4 and Oat_v1. L-Lactate, nicotinate, and pyrazinoate are substrates for the high and low affinity SMCT1 and SMCT2. hOAT10 is speculated to be present in S1/S2 segments because of our Western blot data of rOat10 expression in cortical brush border membrane vesicles. Considering the localization of SMCT1 (no expression in S1, weakly expressed in S2, and highly expressed in S3 segment) and SMCT2, which represents the low affinity lactate and nicotinate transporter (expressed in all three segments) in the proximal tubule, the question arises of whether SMCT1 could be the important player, providing the driving forces for urate uptake via hURAT1 (49). We postulate that SMCT2 provides the lactate gradient for hURAT1 and probably also for hOAT10-mediated urate transport, which might be the main driving force for urate reabsorption in renal proximal tubule cells, because a knock-down of SMCT1 and SMCT2 in CCAAT enhancer-binding protein δ null mice showed reduced lactate levels in plasma and elevated urate levels in the urine (50). Nicotinate may serve as counter ion for urate reabsorption in the proximal tubule only under therapeutic concentrations. Thus, the physiological role of hOAT10 is supposed to be the nicotinate uptake pathway.

Glutarate, which is used as a nondegradable analog of α-ketoglutarate, is a well known exchange anion for several urate transporters such as OAT1, OAT3, and hOAT4 (16, 24). However, preloading of *X. laevis* oocytes with glutarate did not stimulate urate transport by hOAT10, documenting that hOAT10 shares some more properties with hURAT1 than with other urate transporters.

Interestingly, hOAT10 facilitates urate$^-$/succinate^{2-} exchange, but it does not take up succinate from the extracellular side (data not shown). Recently it was found that rat Oat5 exchanges ES against succinate (51). The human ortholog of OAT5 is exclusively expressed in the liver (52), indicating that hOAT10 is the first identified human renal OAT, which uses succinate as a driving force. Consequently, we suggest that hOAT10 is functionally connected to NaDC-1 (sodium dicarboxylate cotransporter 1), which provides the succinate gradient. Succinate was recently identified as a ligand for a G protein-coupled receptor, namely GPR91, which is exclusively expressed in the distal nephron segment especially in macula densa cells (53). High plasma concentrations of succinate result in renin-dependent hypertension, which is reversed in GPR91 null mice, indicating that transporters like hOAT10, which may increase succinate concentration in the primary urine, may play a role in succinate homeostasis in the urine.

hOAT10 shows pH dependence with highest PAH uptakes at pH 5.0, a pH value at which PAH is still in its anionic form, suggesting that hOAT10 additionally supports PAH/OH$^-$ or urate/OH$^-$ exchange and may be therefore possibly coupled with the sodium proton exchanger 3 like hOAT4. Consequently, hOAT10 resembles in some aspects characteristics of both hURAT1 and hOAT4. Classifications of urate transporters by their transport modes and their associated proteins like these are necessary to identify and differentiate in the future those transporters involved in reabsorption and those facilitating the secretion processes of urate in the kidneys.

It has been known for a long time that up to 80% of transplant patients treated with cyclosporine A have hyperuricemia and up to 25% of these develop gout (54). The cyclosporine-induced hyperuricemia is presumed to be due to a decrease in kidney function or even kidney damage. *Trans*-stimulation studies on urate uptake by hOAT10 demonstrate for the first time that secretion of cyclosporine A enhances urate reabsorption, resulting finally in hyperuricemia. Whether cyclosporine A enters the cell from the basolateral side via an OAT, possibly OAT1 or OAT3, is still not known. Hydrochlorothiazide did not alter urate uptake by hOAT10, indicating that this effect is specific for hOAT4 (16).

GSH has been shown to provide protection against the toxic effects of free radicals especially under ischemic conditions and toxins, which normally result in oxidative injury and cellular disruption. The renal proximal tubule cells synthesize and store high amounts (up to 10 mM) of GSH, whereas the plasma concentration of GSH is quite low (10 μM) (55). Luminal secretion of GSH is known to be high in the S1 segment of rabbit kidneys and has been proposed to involve OATP1 (organic anion transporting polypeptide 1) as well as MRP2 and MRP4 (multi-drug resistance-related proteins 2 and 4) (55). hOAT10 exhibited an asymmetric behavior for glutathione handling, because GSH did not alter PAH uptake if it was provided from the *cis*-(luminal) side. However, *trans*-stimulation studies, offering GSH from the cytosolic side, revealed the first evidence that GSH serves as a counter ion for urate reabsorption, releasing GSH into the lumen. Consequently, we suggest that hOAT10 is involved in the luminal glutathione cycle in the kidneys.

In summary, we have identified a new human organic anion transporter, hOAT10, that is a urate and the first known high affinity nicotinate transporter. Moreover, we are able to provide the first molecular evidence for cyclosporine A-induced hyperuricemia because of a hOAT10-mediated increase in urate reabsorption. Finally, the two newly identified substrates (counter ions) of hOAT10 (succinate and glutathione) and their influence on kidney function pave the way for further interesting studies on this transporter.

Acknowledgments—We thank G. Dallmeyer and A. Hillemann for excellent technical assistance and A. Nolte (Department of Biochemistry, Universität Göttingen) for nucleotide sequencing.

REFERENCES

1. Wright, S. H., and Dantzler, W. H. (2004) *Physiol. Rev.* **84,** 987–1049
2. Rizwan, A. N., and Burckhardt, G. (2007) *Pharm. Res.* **24,** 450–470
3. Anzai, N., Kanai, Y., and Endou, H. (2006) *J. Pharmacol. Sci.* **100,** 411–426
4. Hediger, M. A., Romero, M. F., Peng, J. B., Rolfs, A., Takanaga, H., and Bruford, E. A. (2004) *Pfluegers Arch. Eur. J. Physiol.* **447,** 465–468
5. Sweet, D. H., Wolff, N. A., and Pritchard, J. B. (1997) *J. Biol. Chem.* **272,** 30088–30095
6. Sekine, T., Watanabe, N., Hosoyamada, M., Kanai, Y., and Endou, H. (1997) *J. Biol. Chem.* **272,** 18526–18529
7. Wolff, N. A., Werner, A., Burkhardt, S., and Burckhardt, G. (1997) *FEBS Lett.* **417,** 287–291
8. Sekine, T., Cha, S. H., Tsuda, M., Apiwattanakul, N., Nakajima, N., Kanai, Y., and Endou, H. (1998) *FEBS Lett.* **429,** 179–182
9. Kusuhara, H., Sekine, T., Utsunomiya-Tate, N., Tsuda, M., Kojima, R., Cha, S. H., Sugiyama, Y., Kanai, Y., and Endou, H. (1999) *J. Biol. Chem.* **274,** 13675–13680
10. Cha, S. H., Sekine, T., Kusuhara, H., Yu, E., Kim, J. Y., Kim, D. K., Sugiyama, Y., Kanai, Y., and Endou, H. (2000) *J. Biol. Chem.* **275,** 4507–4512
11. Youngblood, G. L., and Sweet, D. H. (2004) *Am. J. Physiol.* **287,** F236–F244
12. Schnabolk, G. W., Youngblood, G. L., and Sweet, D. H. (2006) *Am. J. Physiol.* **291,** F314–F321
13. Shin, H. J., Anzai, N., Enomoto, A., He, X., Kim, d. K., Endou, H., and Kanai, Y. (2007) *Hepatology* **45,** 1046–1055
14. Jutabha, P., Kanai, Y., Hosoyamada, M., Chairoungdua, A., Kim, d. K., Iribe, Y., Babu, E., Kim, J. Y., Anzai, N., Chatsudthipong, V., and Endou, H. (2003) *J. Biol. Chem.* **278,** 27930–27938
15. Enomoto, A., Kimura, H., Chairoungdua, A., Shigeta, Y., Jutabha, P., Ho, C. S., Hosoyamada, M., Takeda, M., Sekine, T., Igarashi, T., Matsuo, H., Kikuchi, Y., Oda, T., Ichida, K., Hosoya, T., Shimokata, K., Niwa, T., Kanai, Y., and Endou, H. (2002) *Nature* **417,** 447–452
16. Hagos, Y., Stein, D., Ugele, B., Burckhardt, G., and Bahn, A. (2007) *J. Am. Soc. Nephrol.* **18,** 430–439
17. Bakhiya, N., Bahn, A., Burckhardt, G., and Wolff, N. (2003) *Cell Physiol. Biochem.* **13,** 249–256
18. Kimura, H., Takeda, M., Narikawa, S., Enomoto, A., Ichida, K., and Endou, H. (2002) *J. Pharmacol. Exp. Ther.* **301,** 293–298
19. Alebouyeh, M., Takeda, M., Onozato, M. L., Tojo, A., Noshiro, R., Hasannejad, H., Inatomi, J., Narikawa, S., Huang, X. L., Khamdang, S., Anzai, N., and Endou, H. (2003) *J. Pharmacol. Sci.* **93,** 430–436
20. Bahn, A., Ljubojevic, M., Lorenz, H., Schultz, C., Ghebremedhin, E., Ugele, B., Sabolic, I., Burckhardt, G., and Hagos, Y. (2005) *Am. J. Physiol.* **289,** C1075–C1084
21. Bahn, A., Knabe, M., Hagos, Y., Rodiger, M., Godehardt, S., Graber-Neufeld, D. S., Evans, K. K., Burckhardt, G., and Wright, S. H. (2002) *Mol. Pharmacol.* **62,** 1128–1136
22. Hagos, Y., Bahn, A., Vormfelde, S. V., Brockmoller, J., and Burckhardt, G. (2007) *J. Am. Soc. Nephrol.* **18,** 3101–3109
23. Hasannejad, H., Takeda, M., Taki, K., Shin, H. J., Babu, E., Jutabha, P., Khamdang, S., Aleboyeh, M., Onozato, M. L., Tojo, A., Enomoto, A., Anzai, N., Narikawa, S., Huang, X. L., Niwa, T., and Endou, H. (2004) *J.*

Pharmacol. Exp. Ther. **308,** 1021–1029
24. Burckhardt, B. C., and Burckhardt, G. (2003) *Rev. Physiol. Biochem. Pharmacol.* **146,** 95–158
25. Nishiwaki, T., Daigo, Y., Tamari, M., Fujii, Y., and Nakamura, Y. (1998) *Cytogenet. Cell Genet.* **83,** 251–255
26. Huang, X. (1994) *Comput. Appl. Biosci.* **10,** 227–235
27. Sindic, A., Hirsch, J. R., Velic, A., Piechota, H., and Schlatter, E. (2005) *Kidney Int.* **67,** 1420–1427
28. Krick, W., Wolff, N. A., and Burckhardt, G. (2000) *Pfluegers Arch. Eur. J. Physiol.* **441,** 125–132
29. Shimada, H., Moewes, B., and Burckhardt, G. (1987) *Am. J. Physiol.* **253,** F795–F801
30. Bradford, M. M. (1976) *Anal. Biochem.* **72,** 248–254
31. Malo, C., and Berteloot, A. (1991) *J. Membr. Biol.* **122,** 127–141
32. Nabokina, S. M., Kashyap, M. L., and Said, H. M. (2005) *Am. J. Physiol.* **289,** C97–C103
33. Anzai, N., Miyazaki, H., Noshiro, R., Khamdang, S., Chairoungdua, A., Shin, H. J., Enomoto, A., Sakamoto, S., Hirata, T., Tomita, K., Kanai, Y., and Endou, H. (2004) *J. Biol. Chem.* **279,** 45942–45950
34. Miyazaki, H., Anzai, N., Ekaratanawong, S., Sakata, T., Shin, H. J., Jutabha, P., Hirata, T., He, X., Nonoguchi, H., Tomita, K., Kanai, Y., and Endou, H. (2005) *J. Am. Soc. Nephrol.* **16,** 3498–3506
35. Ljubojevic, M., Balen, D., Breljak, D., Kusan, M., Anzai, N., Bahn, A., Burckhardt, G., and Sabolic, I. (2007) *Am. J. Physiol.* **292,** F361–F372
36. Ljubojevic, M., Herak-Kramberger, C. M., Hagos, Y., Bahn, A., Endou, H., Burckhardt, G., and Sabolic, I. (2004) *Am. J. Physiol.* **287,** F124–F138
37. Hosoyamada, M., Ichida, K., Enomoto, A., Hosoya, T., and Endou, H. (2004) *J. Am. Soc. Nephrol.* **15,** 261–268
38. Sabolic, I., Asif, A. R., Budach, W. E., Wanke, C., Bahn, A., and Burckhardt, G. (2007) *Pfluegers Arch. Eur. J. Physiol.* **455,** 397–429
39. Bonilla-Felix, M. (2004) *Am. J. Physiol.* **287,** F1093–F1101
40. Takanaga, H., Maeda, H., Yabuuchi, H., Tamai, I., Higashida, H., and Tsuji, A. (1996) *J. Pharm. Pharmacol.* **48,** 1073–1077
41. Gopal, E., Miyauchi, S., Martin, P. M., Ananth, S., Roon, P., Smith, S. B., and Ganapathy, V. (2007) *Pharm. Res.* **24,** 575–584
42. Hara, N., Yamada, K., Shibata, T., Osago, H., Hashimoto, T., and Tsuchiya, M. (2007) *J. Biol. Chem.* **282,** 24574–24582
43. Anzai, N., Enomoto, A., and Endou, H. (2005) *Curr. Rheumatol. Rep.* **7,** 227–234
44. Hediger, M. A., Johnson, R. J., Miyazaki, H., and Endou, H. (2005) *Physiology* **20,** 125–133
45. Kutzing, M. K., and Firestein, B. L. (2008) *J. Pharmacol. Exp. Ther.* **324,** 1–7
46. Eraly, S. A., Vallon, V., Rieg, T., Gangoiti, J. A., Wikoff, W. R., Siuzdak, G., Barshop, B. A., and Nigam, S. K. (2008) *Physiol Genomics* **33,** 180–192
47. Vitart, V., Rudan, I., Hayward, C., Gray, N. K., Floyd, J., Palmer, C. N., Knott, S. A., Kolcic, I., Polasek, O., Graessler, J., Wilson, J. F., Marinaki, A., Riches, P. L., Shu, X., Janicijevic, B., Smolej-Narancic, N., Gorgoni, B., Morgan, J., Campbell, S., Biloglav, Z., Barac-Lauc, L., Pericic, M., Klaric, I. M., Zgaga, L., Skaric-Juric, T., Wild, S. H., Richardson, W. A., Hohenstein, P., Kimber, C. H., Tenesa, A., Donnelly, L. A., Fairbanks, L. D., Aringer, M., McKeigue, P. M., Ralston, S. H., Morris, A. D., Rudan, P., Hastie, N. D., Campbell, H., and Wright, A. F. (2008) *Nat. Genet.* **40,** 437–442
48. Graessler, J., Graessler, A., Unger, S., Kopprasch, S., Tausche, A. K., Kuhlisch, E., and Schroeder, H. E. (2006) *Arthritis Rheum.* **54,** 292–300
49. Gopal, E., Umapathy, N. S., Martin, P. M., Ananth, S., Gnana-Prakasam, J. P., Becker, H., Wagner, C. A., Ganapathy, V., and Prasad, P. D. (2007) *Biochim. Biophys. Acta* **1768,** 2690–2697
50. Thangaraju, M., Ananth, S., Martin, P. M., Roon, P., Smith, S. B., Sterneck, E., Prasad, P. D., and Ganapathy, V. (2006) *J. Biol. Chem.* **281,** 26769–26773
51. Anzai, N., Jutabha, P., Enomoto, A., Yokoyama, H., Nonoguchi, H., Hirata, T., Shiraya, K., He, X., Cha, S. H., Takeda, M., Miyazaki, H., Sakata, T., Tomita, K., Igarashi, T., Kanai, Y., and Endou, H. (2005) *J. Pharmacol. Exp. Ther.* **315,** 534–544
52. Sun, W., Wu, R. R., van Poelje, P. D., and Erion, M. D. (2001) *Biochem. Biophys. Res. Commun.* **283,** 417–422
53. He, W., Miao, F. J., Lin, D. C., Schwandner, R. T., Wang, Z., Gao, J., Chen, J. L., Tian, H., and Ling, L. (2004) *Nature* **429,** 188–193
54. Zurcher, R. M., Bock, H. A., and Thiel, G. (1996) *Nephrol. Dial. Transplant.* **11,** 153–158
55. Frey, I. M., Rubio-Aliaga, I., Siewert, A., Sailer, D., Drobyshev, A., Beckers, J., de Angelis, M. H., Aubert, J., Bar, H. A., Fiehn, O., Eichinger, H. M., and Daniel, H. (2007) *Physiol. Genomics* **28,** 301–310